Noise characteristics of 100 nm scale GaAs/$Al_xGa_{1-x}As$ scanning Hall probes

C. W. Hicks,[a] L. Luan, and K. A. Moler
Geballe Laboratory for Advanced Materials, Stanford University, Stanford, California 94305

E. Zeldov and H. Shtrikman
Department of Condensed Matter Physics, The Weizmann Institute of Science, Rehovot 76100, Israel

(Received 6 November 2006; accepted 24 February 2007; published online 29 March 2007)

The authors have fabricated and characterized GaAs/$Al_xGa_{1-x}As$ two-dimensional electron gas scanning Hall probes for imaging perpendicular magnetic fields at surfaces. The Hall crosses range from 85×85 to 1000×1000 nm^2. They study low-frequency noise in these probes, especially random telegraph noise, and show that low-frequency noise can be significantly reduced by optimizing the voltage on a gate over the Hall cross. The authors demonstrate a 100 nm Hall probe with a sensitivity of 0.5 G/$\sqrt{\text{Hz}}$ (flux sensitivity of $0.25m\Phi_0/\sqrt{\text{Hz}}$; spin sensitivity of $1.2\times10^4\mu_B/\sqrt{\text{Hz}}$) at 3 Hz and 9 K. © *2007 American Institute of Physics*. [DOI: 10.1063/1.2717565]

Magnetic imaging techniques are useful for studying systems with magnetic features at microscopic length scales. Magnetic force microscopy offers the highest spatial resolution currently achievable without special sample preparation, around 30 nm. Hall probes offer the prospect of similar resolution but with a nonperturbative probe that directly measures B_z. In this study we demonstrate Hall probes as small as 100 nm, fabricated in a scanning geometry on GaAs/AlGaAs two-dimensional electron gas (2DEG), and discuss variation of noise characteristics with probe size.

Submicron GaAs/AlGaAs scanning Hall probes have been demonstrated in cryogenic scanning systems,[1–5] including 250 nm probes with ≈300 nm actual resolution when the Hall cross-sample separation is included.[1] 250 nm GaSb/InAs/GaSb scanning probes have also been demonstrated.[5] 50 nm Bi-film Hall crosses have been demonstrated at room temperature.[6] However, Bi film offers poorer sensitivity and is prone to cracking during thermal cycling.[7] Micron-scale Si/SiGe and InGaAs/InP Hall crosses have been characterized at low temperature but have not been incorporated into scanning probes.[8,9]

The Hall signal is $V=I(R_{\text{offset}}+R_HB_z)$, where B_z is the average perpendicular field at the Hall cross, I is the drive current, $R_H=1/ne$ is the Hall coefficient (n is the 2D carrier density), and R_{offset} is due to lithography imperfections or asymmetrical current flow. Useful systems offer low n (for large R_H) and high mobility μ (for higher conductance, reducing Johnson noise, and allowing higher drive current).

Attaining high spatial resolution requires that the Hall cross be small and that it be near the sample surface. On our probes the contact tip is ~1 μm from the Hall cross, so aligning the probe and sample to 1°–3° allows the chip surface above the cross to be brought to 20–50 nm from the sample surface. The thickness and/or depth of the Hall cross material adds to this, so a shallow 2DEG is therefore essential. We use two different GaAs/AlGaAs heterostructures for this study, a 39 nm deep δ-doped structure from IQE plc, Cardiff, UK ("structure A") and a 40 nm deep slab-doped structure grown at the Weizmann Institute of Science ("structure B").[10] We fabricated probes on structure A of sizes of 100 (e.g., Fig. 1), 105, 200, and 350 nm, and on structure B of 85, 100, 130, 180, 230, 390, 500, and 1000 nm. At 4.2 K the structure A 2DEG has $n=3.5\times10^{11}$ cm^{-2} and $\mu=1.4\times10^5$ cm^2/V s, and structure B has $n=5\times10^{11}$ and $\mu=2.5\times10^5$.

The Hall cross is patterned by electron-beam lithography and reactive ion etching (RIE). Aiming for small probes we use thin etch lines (~20 nm wide adjacent to the cross itself for the 100, 150, and 200 nm probes) and a shallow RIE, 29–31 nm deep, through the dopant layer of both structures, sufficient to cut off conduction in the 2DEG beneath at low temperature (we have tested these probes up to 95 K). Tests with gaps of various widths (quantum point contacts) in single 20 nm wide, 35 nm deep etch lines at 4 and 77 K suggest lateral depletion to be ~10 nm. 100 nm probes should then have clear conduction paths after allowing for finite linewidth and lateral depletion, but we find that a significant fraction does not conduct well, suggesting additional depletion.

Two etches form the tip: $a\approx300$ nm deep RIE near the Hall cross and an ≈1 μm wet etch further out. A blanket

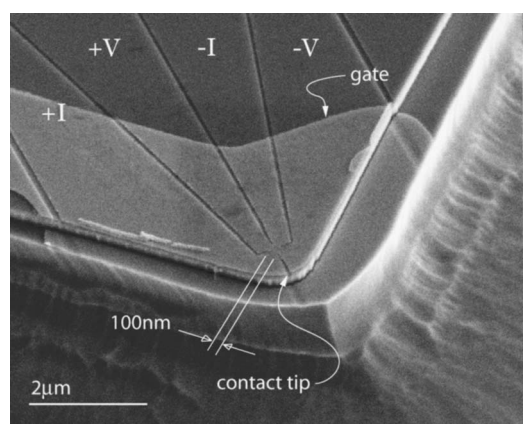

FIG. 1. Scanning electron microscope image of a 100 nm Hall probe on structure A. The four leads are separated by narrow etch lines. The gate shields the Hall cross from stray electrical charges and allows modulation of the 2DEG beneath. The Hall probe will touch the sample surface at the contact tip.

[a]Electronic mail: cwhicks@stanford.edu

 © 2007 American Institute of Physics
Downloaded 24 Oct 2007 to 132.77.4.43. Redistribution subject to AIP license or copyright, see http://apl.aip.org/apl/copyright.jsp

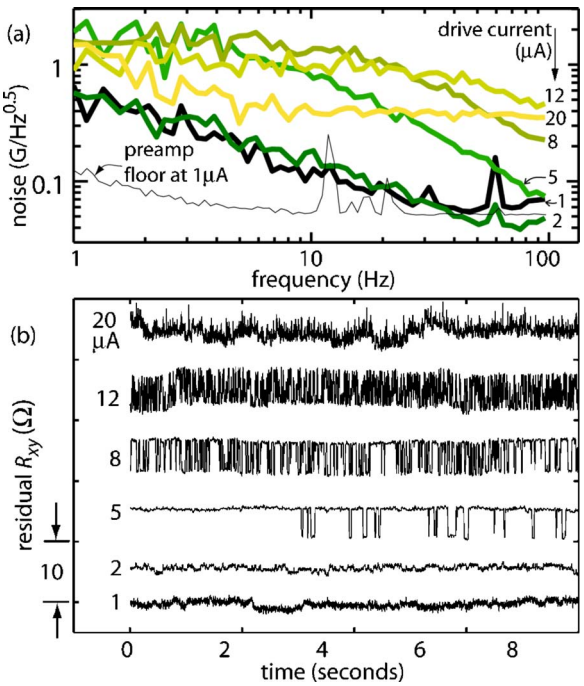

FIG. 2. (Color online) (a) Noise spectra at various drive currents for a structure A 350 nm probe at 4.2 K with $V_g=0$. Each spectrum is based on 30 s of data. Preamp noise floor recorded with the probe connected but no drive current and converted to ohms taking $I=1$ μA. R_H are (units are μA:Ω/G) 1: 0.201, 2: 0.207, 5: 0.184, 8: 0.189, 12: 0.184, and 20: 0.172. (b) Time traces for the spectra in (a). The signal from a 40 G_{pp}, 0.04 Hz applied field (for determining R_H) has been subtracted.

gate deposited on most probes shields against stray electric charges during scanning; all structure A probes are gated (12 nm Ti+10 Au) but only the 500 nm structure B probe is gated (5 nm Ti+10 Au).

We drive the probes with a dc I while continuously applying a 40 G_{pp}, 0.04 Hz field for determination of R_H. We record the Hall voltage for 100 s at each I and gate voltage V_g (with V_g measured relative to the Hall cross 2DEG). With one exception (noted below) the probes were cooled with $V_g=0$.

Figure 2(a) shows field equivalent noise, $S_B^{1/2}$, from a 350 nm probe with various I, and Fig. 2(b) shows the corresponding time traces. $S_B^{1/2}=S_R^{1/2}/R_H(I)=S_V^{1/2}/IR_H(I)$, where S_R and S_V are the resistance and voltage noise power spectral densities. R_H typically varies slightly with I. Random telegraph noise (RTN) is common in small semiconductor devices;[11,12] a clear example is visible in the $I \geqslant 5$ μA time traces of Fig. 2(b). The power spectrum of RTN is[13]

$$S_R(f) = \frac{(R_2 - R_1)^2}{\tau_1 + \tau_2}\left(\frac{1}{\tau^{-2} + (2\pi f)^2}\right),$$

where τ_1 and τ_2 are the lifetimes of the two states, R_1 and R_2 their resistances, and $\tau^{-1}=\tau_1^{-1}+\tau_2^{-1}$. If the activation energies of multiple thermally activated RTN processes are uniformly distributed, the distribution of lifetimes is $1/\tau$. If spectra from multiple independent sources so distributed are added, the result is a $1/f$ spectrum,[14] such that discrete switching noise in small devices evolves into $1/f$ noise in larger devices. The curved 5, 8, and 12 μA spectra shown in Fig. 2(a) are typical when one RTN source dominates.

The 1 and 2 μA spectra in Fig. 2(a) are nearly identical. Sometimes a RTN source active at low I turns off with increasing I, but the scenario in Fig. 2 is more typical: nearly constant *resistance* noise at low I, then a jump when one or more RTN sources activate at larger I. Constant resistance noise means that a larger or ac I does not improve the intrinsic sensitivity of the Hall probe. The activation of RTN with increasing drive current is probably a hot-electron effect: the thermal conductivity of GaAs below 50 K is $\sim$10 W/K cm^2,[15] so to heat the lattice around even a 100 nm probe from, e.g., 4 to 10 K would require a current of $\sim$300 μA ($R_{xx}\sim$10 kΩ for a 100 nm probe and $\sim$1 kΩ for 1 μm).

The amplitude of individual RTN signals, in ohms, is usually nearly constant in I. We observe no correlation with B up to 20 G, suggesting that RTN primarily affects R_{offset}, by modifying the scattering (the mobility) in the Hall cross. Measurements on a 1 μm structure B probe showed no change in amplitude up to 600 G. However, over the range of $0<B<1$ T, $S_R^{1/2}$ has been reported to scale with B, suggesting that RTN does also affect n.[11,16] If RTN affects n and R_{offset} simultaneously, then the n fluctuations would be the more visible at large fields where $\delta(R_H B)=(\delta n/en^2)B$ becomes larger than $\delta(R_{\text{offset}})$.

The amplitude of RTN grows rapidly for probes smaller than $\sim$500 nm: the largest RTN amplitudes we saw in gated probes in this study are 500 nm: 0.4 Ω, 350 nm: 3.5 Ω, 200 nm: 1.5 and 36 Ω, 150 nm: 9.6, 14, and 57 Ω, and 100 nm: 5, 90, and 100 Ω. (Each datum is a different probe or a different cooldown of the same probe. All except the 500 nm are structure A probes.) Minimizing RTN by adjusting I or V_g becomes essential. Optimization of I usually means setting I to a point somewhat below activation of additional RTN sources. For 100–500 nm probes this can

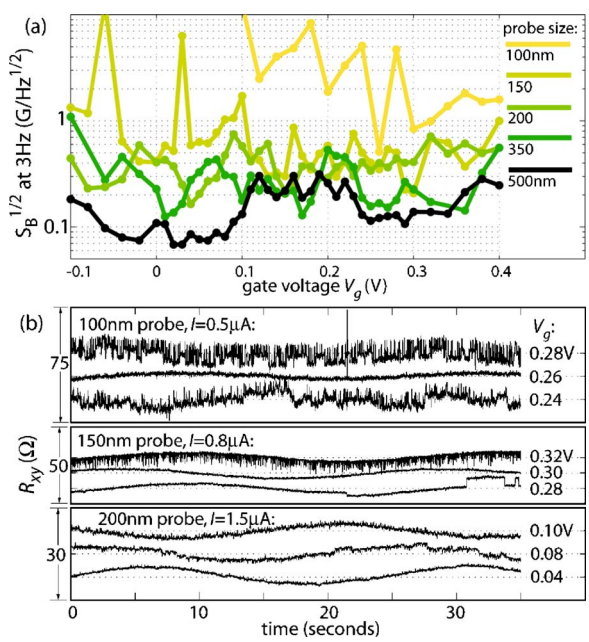

FIG. 3. (Color online) (a) $S_B^{1/2}$ of various probes vs V_g at 8.7 K. V_g was stepped from −0.1 to +0.4 V in 0.01 or 0.02 V increments while maintaining I continuously. Each point is based on 100 s of data. 500 nm probe: structure B; all others: A. (b) Time traces for some of the points in (a); traces offset for clarity. The slow oscillation is a 40 G_{pp} 0.04 Hz applied field for determining R_H. Drive currents are [probe (nm): μA] 100: 0.5, 150: 0.8, 200: 1.5, 350: 2, and 500: 2. Cooldown gate voltage V_{gc} was −0.3 V for the 100 nm probe and 0 otherwise.

Downloaded 24 Oct 2007 to 132.77.4.43. Redistribution subject to AIP license or copyright, see http://apl.aip.org/apl/copyright.jsp

fall in a large range, ~1–10 μA, suggesting a variety of source configurations.

Figure 3 shows $S_B^{1/2}$ vs V_g over $-0.1 < V_g < 0.4$ V for probes of various sizes. The thresholds V_g to deplete the 2DEG entirely are ≈−0.2 V and ≈−0.3 V for structures A and B, respectively; we find that sensitivity usually degrades rapidly for $V_g < -0.1$ V. The upper limit on V_g is set by leakage over the surface Schottky barrier, ~1 nA at 0.5 V and ~1 μA at 0.6 V.

Small variations in V_g (as small as 10 mV below ~10 K) can vary $S_B^{1/2}$ by several hundred percent, especially for smaller probes. For example, in Fig. 3 the 100 nm probe is particularly quiet at $V_g = 0.26$ V, but considerably less so at 0.24 and 0.28 V. It has been reported that, at $T = 45$ K and $B = 0.5$ T and for Hall crosses of sizes between 0.45 and 5 μm, $V_g > \approx 100$ mV suppresses $S_R^{1/2}$ by roughly an order of magnitude from $V_g = 0$.[16,17] We do not find such a clear pattern; rather, working at $T < 10$ K and $B \leqslant 20$ G, we find that the precise points in V_g where RTN is suppressed vary from probe to probe.

We studied three probes (200, 350, and 500 nm) at various T between 4.2 and 77 K. At 37 K a variation $\Delta V_g = 0.01$ V could still activate or deactivate a RTN source, while at 77 K the transitions widened to $\Delta V_g \sim 0.05$ V. The base noise level did not increase.

For the 100 nm probe data in Fig. 3 we applied a gate voltage during cooldown (V_{gc}) of −0.3 V. This increases the number of dopants that ionize at 300 K and, when V_g is returned to $\geqslant 0$ at low temperature, additional mobile electrons are drawn into the dopant layer.[18] The effect is akin to freezing in an offset to V_g: $V_{gc} = -0.3$ V and $V_g = +0.3$ V give an effective V_g of ≈0.6 V. Compared with an earlier $V_{gc} = 0$ run, R_{xx} was ≈10% lower and sensitivity about twice as good.

Figure 4 shows $S_B^{1/2}$ at 3 Hz obtained with optimization by varting I *or* V_g for various probes. We choose 3 Hz as it is comparable to typical scan speeds, ~1 s per line, but not excessively slow to measure. The data strongly suggest that tuning V_g at a preselected I is a more useful exercise than tuning I at $V_g = 0$.

Smaller probes show higher $S_B^{1/2}$; however, if one converts to flux noise by multiplying by Hall cross area the small probes are more sensitive (500 nm probe: $7 \times 10^{-4} \Phi_0/\sqrt{\text{Hz}}$; 100 nm probe: 2.5×10^{-4}). Spin sensitivity gains further:[19] it is $2.2 \times 10^5 \mu_B/\sqrt{\text{Hz}}$ for the 500 nm and 1.2×10^4 for the 100 nm probe if the moment is placed at half the cross width above the center of the Hall cross.

What can we learn about the sources of RTN? The activation energies for noise from *DX* centers are too large to be relevant at ~10 K.[20] Cobden *et al.*, using a 100 nm deep 2DEG, identify low-temperature RTN sources as electrons hopping between defect sites at various depths between surface gates and the 2DEG.[12] If a 10 mV shift in V_g can activate or deactivate a RTN source, it is presumably by shifting the relative energies of two defect sites by a few times $k_B T$. At 8.7 K, $k_B T = 0.75$ meV, implying a shift of perhaps 3 meV or a vertical separation of ~30% of the gate-2DEG distance. Our data are consistent with the scenario of Cobden *et al.*

In summary, we find that GaAs/$Al_xGa_{1-x}As$ Hall probes can be made with active areas as small as 100 nm and sensitivities of a few Gauss. Tuning the gate voltage can significantly improve sensitivity, particularly for smaller probes, and is more effective than tuning the drive current.

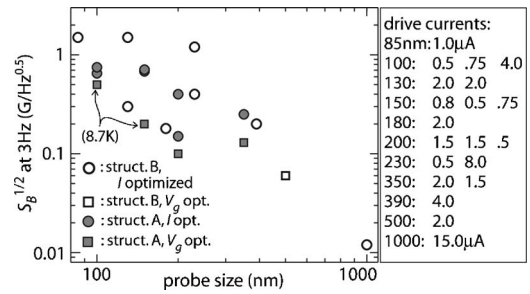

FIG. 4. Partially optimized field equivalent noise at 3 Hz. Each point is a separate cooldown; $T = 4.2$ K except where noted. Circles: optimized by varying I, with the gate absent or $V_g = 0$. Squares: optimized by varying V_g at preselected currents; V_g for each square (units are nm: V): 100: 0.26, 150: 0.30, 200: −0.02, 350: 0.02, and 500: −0.06. Drive currents in the table are listed from the bottom up where there are multiple points at one size.

For assistance with fabrication the authors are grateful to the staff at the Stanford Nanofabrication Facility. They also thank David Goldhaber-Gordon and Yuri Myasoedov for useful discussions. The authors also acknowledge funding support from the Department of Energy (DE-AC02-76SF00515), the NSF Center for Probing the Nanoscale (PHY-0425897), and the US-Israel Binational Science Foundation.

[1] A. Oral, J. C. Barnard, S. J. Bending, I. I. Kaya, S. Ooi, T. Tamegai, and M. Henini, Phys. Rev. Lett. **80**, 3610 (1998).
[2] A. Oral, S. J. Bending, and M. Henini, Appl. Phys. Lett. **69**, 1324 (1996).
[3] R. B. Dinner, M. R. Beasley, and K. A. Moler, Rev. Sci. Instrum. **76**, 103702 (2005).
[4] A. M. Chang, H. D. Hallen, L. Harriott, H. F. Hess, H. L. Kao, J. Kwo, R. E. Miller, R. Wolfe, J. van der Ziel, and T. Y. Chang, Appl. Phys. Lett. **61**, 1974 (1992).
[5] A. N. Grigorenko, S. J. Bending, J. K. Gregory, and R. G. Humphreys, Appl. Phys. Lett. **78**, 1586 (2001).
[6] A. Sandhu, K. Kurosawa, M. Dede, and A. Oral, Jpn. J. Appl. Phys., Part 1 **43**, 777 (2004).
[7] E. Pugel, E. Shung, T. F. Rosenbaum, and S. P. Watkins, Appl. Phys. Lett. **71**, 2205 (1997).
[8] R. G. van Veen, A. H. Verbruggen, E. van der Drift, S. Radelaar, S. Anders, and H. M. Jaeger, Rev. Sci. Instrum. **70**, 1767 (1999).
[9] V. Cambel, G. Karapetrov, P. Eliáš, S. Hasenöhrl, W. K. Kwok, J. Krause, and J. Maňka, Microelectron. Eng. **51–52**, 333 (2000).
[10] Structure A: 1 μm GaAs buffer layer+20 nm, $Al_{0.3}Ga_{0.7}As+\delta$ layer +4 nm AlGaAs+δ layer+9 nm AlGaAs+5 nm GaAs cap. Each δ layer is 0.5 nm GaAs+5×10^{12} cm^{-2} Si. Structure B: 500 nm GaAs buffer layer +10 nm $Al_{0.35}Ga_{0.65}As$+15 nm 5×10^{18} cm^{-3} Si-doped AlGaAs+5 nm AlGaAs+10 nm GaAs cap.
[11] Ç. Kurdak, C.-J. Chen, D. C. Tsui, S. Parihar, S. Lyon, and G. W. Weimann, Phys. Rev. B **56**, 9813 (1997).
[12] D. H. Cobden, A. Savchenko, M. Pepper, N. K. Patel, D. A. Ritchie, J. E. F. Frost, and G. A. C. Jones, Phys. Rev. Lett. **69**, 502 (1992).
[13] S. Machlup, J. Appl. Phys. **25**, 341 (1954).
[14] A. L. McWhorter, *Semiconductor Surface Physics* (University of Philadelphia Press, Philadelphia, 1957), pp. 207–228.
[15] S. Adachi, *Properties of Gallium Arsenide*, 3rd ed. (Institution of Electrical Engineers, London, 1996), pp. 32–48.
[16] Y. Li, C. Ren, P. Xiong, S. von Molnár, Y. Ohno, and H. Ohno, Phys. Rev. Lett. **93**, 246602 (2004).
[17] J. Müller, S. von Molnár, Y. Ohno, and H. Ohno, Phys. Rev. Lett. **96**, 186601 (2006).
[18] Brief illumination with a light-emitting diode (LED) at low temperature also creates mobile electrons in the dopant layer. We did not use a LED in this study.
[19] M. B. Ketchen and J. R. Kirtley, Radio Sci. **5**, 2133 (1995).
[20] J. R. Kirtley, T. N. Theis, P. M. Mooney, and S. L. Wright, J. Appl. Phys. **63**, 1541 (1988), and references therein.

Downloaded 24 Oct 2007 to 132.77.4.43. Redistribution subject to AIP license or copyright, see http://apl.aip.org/apl/copyright.jsp